ELSEVIER

Journal of Nuclear Materials 307–311 (2002) 763–768

journal of nuclear materials

www.elsevier.com/locate/jnucmat

Long-term high temperature oxidation behavior of ODS ferritics

B.A. Pint *, I.G. Wright

Metals and Ceramics Division, Oak Ridge National Laboratory, P.O. Box 2008, Oak Ridge, TN 37831-6156, USA

Abstract

Four oxide dispersion strengthened Fe–(13–14 at.%) Cr ferritic compositions were exposed in air and air with 10 vol.% water vapor for up to 10 000 h at 700–1100 °C. At 700–800 °C in air, the reaction rates were very low for all of the alloys compared to stainless steels. At 900 °C, a dispersion of Y_2O_3, compared to Al_2O_3, showed a distinct benefit in improving the oxidation resistance, due to a reactive element effect. However, failure occurred after 7000 h at 900 °C when only 13% Cr was present. The absence of Ti and W in one alloy appeared to result in a thinner reaction product after oxidation at 800 °C. One composition was exposed in 10 vol.% water vapor at 800 and 900 °C and in air at 1000 and 1100 °C. Under both of these conditions, there was a significant increase in the rates of oxidation. With the relatively low Cr contents in these alloys, their corrosion-limited operating temperature in air is near 900 °C.

1. Introduction

There are three major classes of structural materials considered for fusion reactors: ferritic–martensitic steels, vanadium alloys and SiC composites. Each class has its strengths and weaknesses. Vanadium alloys are susceptible to environmental embrittlement by oxygen and hydrogen [1,2] and to low temperature radiation embrittlement [3]. SiC has limitations associated with ceramics of fabrication and lack of engineering design data [4], and ferritic steels are limited in temperature (≈550 °C) due to creep strength [5]. One way to increase the temperature capability of ferritic steels is by incorporation of an oxide dispersion. Mechanical alloying or powder blending techniques to incorporate an oxide dispersion has worked in a wide range of metals [6–8]. For ferritic alloys, the addition of a Y_2O_3 dispersion is most widely known in FeCrAl-type materials (commercial alloys such as Special Metals' MA956 and Plansee's PM2000) which have the best combination of high-temperature strength and oxidation resistance of any material.

Oxide dispersion strengthened (ODS) FeCr alloys also have been investigated [9–13] and these compositions are attractive to fusion applications (as well as fossil energy applications) where the oxide dispersion could significantly boost the creep strength and allow operation at higher temperatures where efficiencies would be more economically attractive. The Fe–Cr matrix compositions are known to resist radiation-induced swelling and have good thermal conductivity. One of the remaining issues is the environmental resistance of these materials. While the addition of oxide dispersions has long been found to improve the corrosion resistance of most Fe- and Ni-base alloys [9,10,14–17], the materials of interest in this study have lower Cr contents (13–14 at.% Cr) than those previously investigated which could limit their ability to form a protective, external Cr_2O_3-rich scale. The objective of these experiments was to examine the long-term, high-temperature (700–1100 °C) oxidation behavior of ODS Fe–Cr alloys to obtain baseline reaction rates.

* Corresponding author. Tel.: +1-423 576 2897/+1-865 576 2897; fax: +1-865 576 28975/241 0215.

E-mail address: pintba@ornl.gov (B.A. Pint).

0022-3115/02/$ - see front matter
PII: S0022-3115(02)01223-0

2. Experimental

The chemical compositions of the four ODS alloys are given in Table 1. Alloys FCW-Y and FCW-Al were supplied by Sumitomo Corp. and contain dispersions of Y_2O_3 and Al_2O_3, respectively. Alloys FC-Y and FCW-YT were supplied by Kobe Steel and contained dispersions of Y_2O_3 and Y_2O_3–TiO_2, respectively. For comparison, three commercially available austenitic alloys also were tested: type 347 stainless steel (18% Cr), type 310 stainless steel (25% Cr) and NF709 (Fe–20Cr–25Ni + Nb). Coupons with 3–5 cm^2 of surface area were made of each composition and polished to a 0.3 μm finish. Prior to oxidation, the specimens were cleaned in acetone and methanol. Oxidation experiments in air were conducted with specimens in individual annealed alumina crucibles with lids in order to obtain the total mass change including spalled or evaporated oxide [18]. Oxidation kinetic data in air were generated by weighing every 100 h (1000–1100 °C) or 500 h (700–900 °C) to total times of 1000–10 000 h using a Mettler model AG245 balance. Oxidation exposures also were conducted in air with 10 ± 1 vol.% H_2O in sealed alumina tubes with a water injection system described elsewhere [19]. Specimens were held in slots in an alumina boat in the furnace hot zone. After these various exposures, selected specimens were examined in plan-view by field-emission gun, scanning electron microscopy and/or Cu-plated and sectioned for metallographic analysis and electron probe microanalysis (EPMA).

Table 1
Chemical compositions of the ferritic ODS alloys in atomic percent

Element	Alloy			
	FCW-Y (EXP)	FC-Y (NOM)	FCW-YT (NOM)	FCW-Al (EXP)
Fe	83.1	86.9	85	80.6
Cr	14.2	12.8	13	14.3
W	0.9		0.9	0.9
Y	0.12	0.12	0.13	<0.01
Ti	0.37		0.47	0.01
Al	0.03			3.3
Si	0.10			<0.10
Ni	0.03			0.06
Mn	0.03			0.01
O	0.76			0.73
N	0.07			0.06
C	0.23			0.05
S (ppma)	114			129

Some of the values are nominal (marked NOM) while others have been confirmed experimentally (EXP) by induction coupled plasma analysis and combustion analysis.

3. Results and discussion

3.1. Reaction kinetics

Figs. 1 and 2 show the mass changes for the various alloys at 700 and 800 °C during 500 h cycles in air. These data were used to calculate [20] steady-state parabolic rate constants, Table 2. For comparison, data and rates for three austenitic stainless steels and ODS FeCrAl (MA956) and ODS NiCr alloy (MA754) are included. At 700 °C, FC-Y and FCW-Al initially showed higher mass gains like the stainless steels but subsequently showed rate constants similar to the other ODS alloys, Table 2. These two alloys (FC-Y and FCW-Al) also

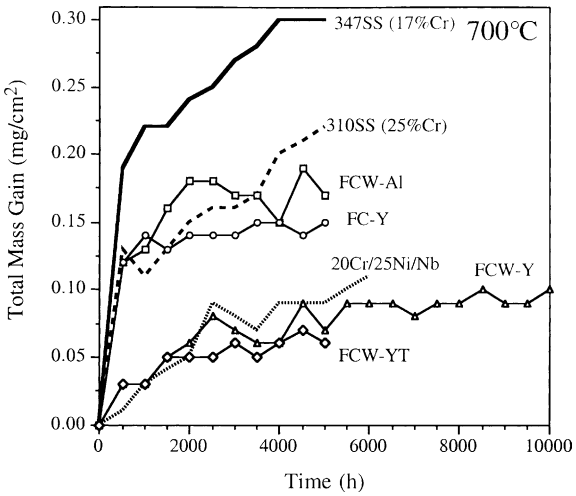

Fig. 1. Total mass gains measured during 500 h cycles in air at 700 °C for the ODS ferritic alloys and several reference alloys.

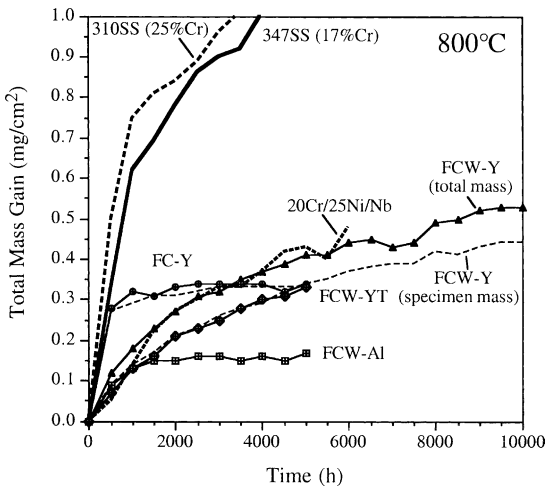

Fig. 2. Total mass gains measured during 500 h cycles in air at 800 °C for the ODS ferritic alloys and several reference alloys.

Table 2
Parabolic rate constants (g^2/cm^4 s) calculated from oxidation data in air

Alloy	Temperature			
	700 °C	800 °C	900 °C	1000 °C
FCW-Y	1.9×10^{-16}	7.1×10^{-15}	6.3×10^{-14}	2.1×10^{-10}
FC-Y	1.2	0.24	–	–
FCW-YT	2.2	8.0	5.9×10^{-14}	–
FCW-Al	2.8	0.75	2.8×10^{-12}	–
Type 347	13	59	–	–
Type 310	8.8	37	–	–
Fe–20Cr–25Ni + Nb	7.2	14	–	–
MA754 (ODS Ni–20Cr)	–	1.6	4.0×10^{-14}	1.0×10^{-12}
MA956 (ODS Fe–20Cr–10Al)	1.9	1.8	1.9×10^{-14}	5.8×10^{-14}

exhibited different behavior from the other alloys at 800 °C. FC-Y showed a very high initial mass gain followed by little additional mass gain. FCW-Al showed the lowest mass gain of any of the alloys at 800 °C. This was likely due to the Al addition (3.3 at.%) slowing the rate of Cr_2O_3 formation or possibly the formation of an Al_2O_3 protective layer, which has a slower rate of growth than Cr_2O_3. Low levels of Al have previously been reported to improve the oxidation resistance of Cr_2O_3-forming alloys [21]. However, it was reported that higher Al levels (>4 at.%) were required to form a continuous Al_2O_3 layer on wrought Fe–Cr–Al alloys [22].

Both the total and specimen mass gains for FCW-Y at 800 °C are shown in Fig. 2. The difference between the two curves is attributed to the volatilization of CrO_3 from the specimen, as the inside of the crucible turned green, and no spalled oxide was found in the bottom of the crucible. The other ODS alloys did not exhibit as much evaporation and thus showed somewhat lower total mass gains. When the oxide scale evaporates, higher oxidation rates are expected since the evaporative thinning of the surface scale reduces the diffusion distance through the oxide compared to a more stable oxide.

Fig. 3 shows the oxidation data obtained at 900 °C. The very high mass gains for FCW-Al after 500 h and for FCW-YT after 7000 h in air reflect breakaway oxidation, i.e. the rapid formation of iron oxide, when the metal becomes depleted in Cr. In contrast, FCW-Y showed no accelerated attack after 10 000 h in air. The difference in performance is somewhat surprising because the FCW-Y specimen was only 1 mm thick while the FCW-Al specimen was 1.4 mm and FCW-YT was 2.4 mm thick. The lower Cr content (13%) in FCW-YT compared to the other two materials may explain its early failure, however, it was much thicker indicating that a standard reservoir model used for predicting lifetime of alumina-forming ODS alloys [23] may not be applicable for these materials. Up to 7000 h, FCW-Y and FCW-YT exhibited similar reaction rates, Table 2.

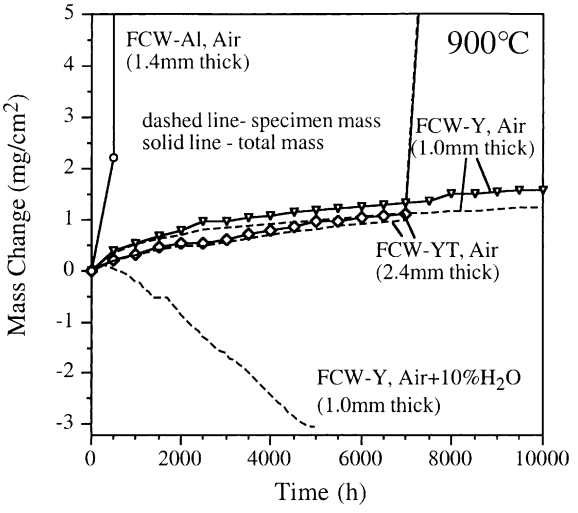

Fig. 3. Total (—) and specimen (- - -) mass gains measured at 900 °C in air and air with 10% water vapor. The specimen thickness is shown for each. The addition of water vapor to the test resulted in mass losses for FCW-Y compared to exposure in air.

The FCW-Al specimen showed a very high reaction rate during the first 500 h in air and subsequently went into breakaway oxidation during the next cycle, Fig. 3. The less protective behavior of FCW-Al was attributed to the absence of Y in this material, as it had the same Cr content as FCW-Y and was thicker (1.4 mm). It is well known that an addition of Y reduces the growth rate of Cr_2O_3 by a factor of 10–100 at this temperature [9,10,21,24,25]. The faster growing scale on FCW-Al (compare the mass gain after one cycle to FCW-Y) consumed more Cr in this alloy and likely caused depletion near the metal–scale interface. No scale spallation was measured after one cycle but any cracking of the scale could have caused rapid reoxidation during the next cycle, sending the alloy into breakaway oxidation.

The addition of 10 vol.% water vapor showed a significant effect on the performance of FCW-Y in 100 h cycles at 900 °C (Fig. 3) and at 800 °C (Fig. 4). The specimen mass losses were attributed to volatilization of $CrO_2(OH)_2$ which can result in accelerated corrosion attack [19,26]. No total mass gains were measured because the covered crucible technique cannot be used in water vapor but the large specimen mass loss would suggest a much faster Cr-consumption rate compared to that in air. These results suggest that further testing will be required if these alloys are expected to experience exposure to water-containing environments in service, even at lower temperatures. Increased pressures and higher flow rates would further exacerbate this problem.

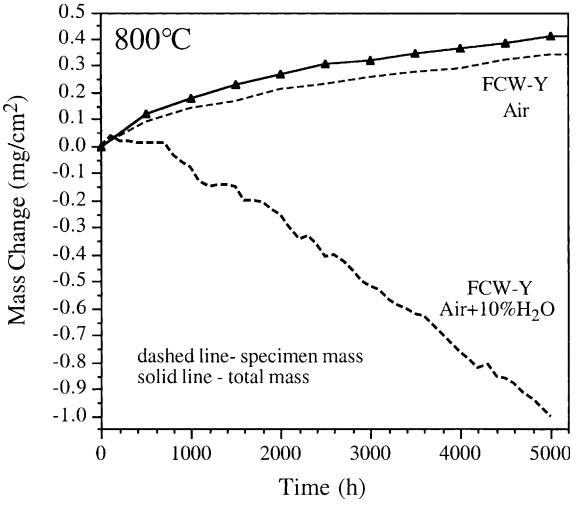

Fig. 4. Total (—) and specimen (- - -) mass gains measured at 800 °C in air and air with 10% water vapor. The addition of water vapor to the test resulted in mass losses for FCW-Y compared to exposure in air.

FCW-Y also was exposed for 10, 100 h cycles at 1000 °C and for 100 h at 1100 °C in air. The parabolic rate constant at 1000 °C was compared to that of two other ODS alloys, Special Metals' Ni–20Cr (MA754) and Fe–20Cr–10Al (MA956) which are known to form protective scales at this temperature [15,16], Table 2. Compared to chromia-forming MA754, FCW-Y showed a 200× higher oxidation rate at 1000 °C indicating that the alloy was not forming a protective external scale as at 900 °C, Table 2. At 1100 °C, a 1.5 mm thick FCW-Y specimen was fully consumed after 100 h.

3.2. Characterization

Metallographic cross-sections of the oxide scales formed on FCW-Y are shown in Fig. 5. The thicknesses of the oxide corresponded well with the mass gains in Figs. 1–3. At the higher temperatures, the metal–scale interface appeared to roughen, possibly due to growth stresses in the oxide. Also, there appeared to be a sig-

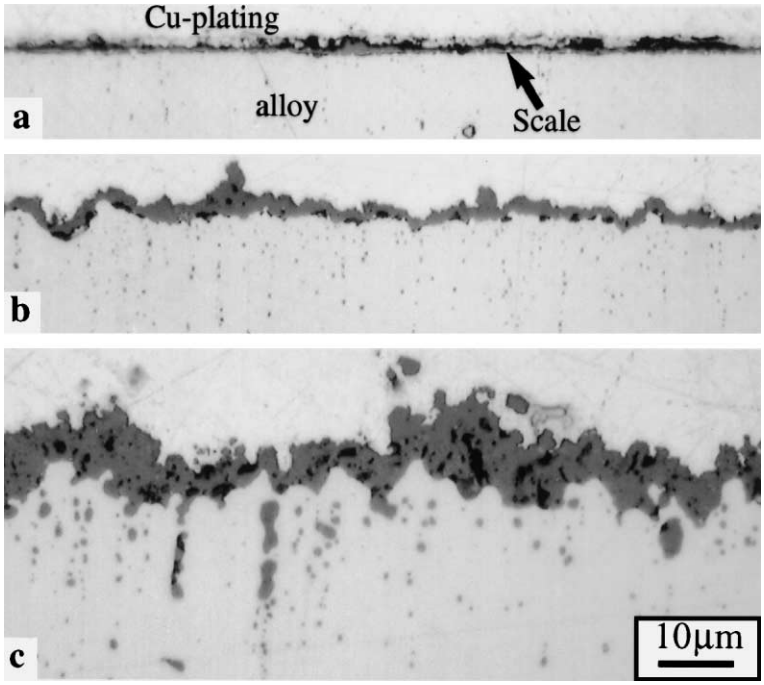

Fig. 5. Light microscopy of polished sections of FCW-Y after 10 000 h exposures in air at (a) 700 °C, (b) 800 °C and (c) 900 °C.

nificant increase in the amount of internal oxide with increasing temperature. The internal oxide was likely rich in Cr, which would have further depleted the Cr reservoir in the metal. There appeared to be pores in the scale formed at 900 °C (Fig. 5(c)); however, these could have been caused by pullouts of fine oxide grains during polishing.

Fig. 6 shows examples of the scales formed on FC-Y, FCW-YT, and FCW-Al after exposures at 700 and 800 °C. The scale on FC-Y after 5000 h at 700 °C showed some Fe-rich nodule formation, indicated by arrows in Fig. 6(a). This is consistent with the high initial mass gain for this alloy, Fig. 1. The fact that the mass gain did not increase as rapidly after the first 500 h suggests that the nodules did not continue to grow during exposure. The reason for nodule formation may be the presence of inhomogeneities in the alloy composition (areas of low Cr), or due to the slightly lower overall Cr content in this alloy, Table 1. Similar behavior was observed at 800 °C, where some very large (50–100 μm) nodules formed, which again corresponded with the high initial mass gain, Fig. 2. Away from the nodules, the scale was very thin (Fig. 6(b)) compared to that formed on FCW-Y (Fig. 5(b)) or the other alloys. The thinner scale resulted in a lower steady-state parabolic rate constant (which does not include the transient nodule formation), Table 2. The reason for the thinner scale may be the absence of Ti in this alloy. The incorporation of Ti in the scale may accelerate the growth of the scale, as Ti has been shown to dope the Cr_2O_3 grains as well as to segregate to the grain boundaries [25]. While Ti is added for mechanical strengthening [11], it may have a slightly negative effect on the oxidation resistance. This alloy also does not contain W, but this refractory metal addition is not likely to have a major effect on oxidation resistance.

The specimen with the Al/Al_2O_3 addition showed higher amounts of internal oxidation after 5000 h at 700 °C than any of the other specimens, Fig. 6(c). This may have been due to the Al content being below the critical level required to form a continuous layer, so that instead it was internally oxidized during the exposure. Oxide particles in the metal also may have resulted from growth of the dispersed Al_2O_3 during exposure. One reason that Y_2O_3 dispersions work well is that the low solubility of Y in the matrix inhibits particle coarsening by Ostwald ripening. After 5000 h at 800 °C, the scale formed on FCW-Al was more uniform.

Compared to FCW-Y, the scale on FCW-YT appeared somewhat different as the oxidation faces were aligned differently to the extrusion direction. The large faces of the FCW-Y coupon were normal to the extrusion direction while those on FCW-YT were parallel to it. The oxide particles in the metal reflect this difference. This may be the reason why the scale was somewhat flatter on FCW-YT, Fig. 6(d). However, this section was made after a 5000 h exposure, whereas that for FCW-Y (Fig. 5(b)) was after 10 000 h. For FCW-YT at 800 °C, the interface appeared to be somewhat rough with a

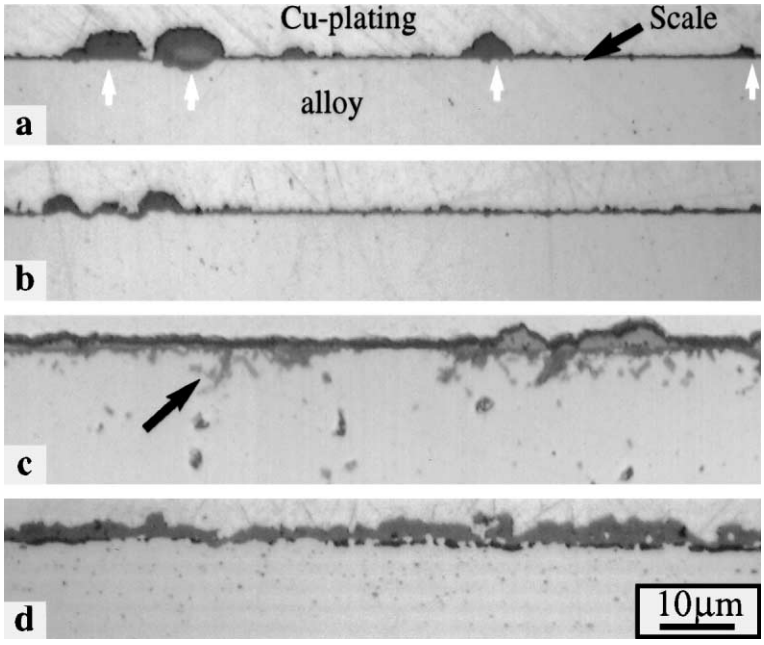

Fig. 6. Light microscopy of polished sections after 5000 h exposures in air of (a) FC-Y at 700 °C, (b) FC-Y at 800 °C, (c) FCW-Al at 700 °C and (d) FCW-YT at 800 °C. Arrows in (a) mark Fe-rich oxide nodules. Arrow in (c) marks internal oxidation.

darker sub-layer adjacent to the substrate, Fig. 6(d). This layer was found to be silica by EPMA. Previous TEM work on FCW-Y showed the presence of a thin (<0.5 μm) silica-layer at the Cr_2O_3–metal interface [27]. that was not observed by light-optical microscopy, Fig. 5. The presence of a silica layer on FCW-Y was unexpected as the Si content is only 0.1 at.%. The thicker silica layer on FCW-YT suggests a higher Si content, unfortunately, the Si content of this material is not known and there was not enough material available for a full chemical analysis.

Overall, these observations indicate that the ODS Fe–Cr alloys follow well-known oxidation behavior. However, the 13–14% Cr in these alloys is a relatively low level for forming a protective Cr_2O_3 scale at high temperatures. The low Cr contents limited the performance of FCW-Y at 1000 °C and FCW-YT and FCW-Al at 900 °C. Previous work on ODS Fe–21% Cr showed good oxidation resistance at 1100 °C when a Y_2O_3 or La_2O_3 dispersion was present [10]. If these materials are intended to be used at temperatures higher than 800 °C, the Cr content needs to be kept as high as possible. Also, conditions which cause oxide erosion or evaporation such as water vapor or high gas velocity will further limit the expected lifetime of this class of alloys.

4. Summary

Four ODS ferritic compositions were tested for up to 10 000 h at 700–1100 °C. At 700–800 °C in air, the reaction rates were very low for all of the alloys compared to commercial stainless steels. At 900 °C, the addition of Y_2O_3, compared to Al_2O_3, showed a distinct benefit in improving the oxidation resistance, due to a reactive element effect. However, a composition with only 13% Cr failed after 7000 h at 900 °C. The absence of Ti and W in one alloy appeared to result in a thinner reaction product after oxidation at 800 °C. One composition was tested in 10% water vapor at 800 and 900 °C and in air at 1000 and 1100 °C. Under these higher temperature conditions, there was a significant increase in the rates of oxidation. With only 13–14 at.% Cr in these alloys, their corrosion-limited operating temperature in air is approximately 900 °C.

Acknowledgements

The research was sponsored by the Office of Fusion Energy Sciences, US Department of Energy (DOE), under contract DE-AC05-00OR22725 with UT-Battelle, LLC. G. Garner, L. Walker and H. Longmire assisted with the experimental work. P.F. Tortorelli and S.J. Zinkle provided comments on the manuscript.

References

[1] J.R. DiStefano, B.A. Pint, J.H. DeVan, H.D. Röhrig, L.D. Chitwood, J. Nucl. Mater. 283–287 (2000) 841.
[2] B.A. Pint, J.R. DiStefano, these Proceedings.
[3] R.J. Kurtz, K. Abe, V.M. Chernov, V.A. Kazakov, G.E. Lucas, H. Matsui, T. Muroga, G.R. Odette, D.L. Smith, S.J. Zinkle, J. Nucl. Mater. 283–287 (2000) 70.
[4] A. Hasegawa, A. Kohyama, R.H. Jones, L.L. Snead, B. Riccardi, P. Fenici, J. Nucl. Mater. 283–287 (2000) 128.
[5] R.L. Klueh, K. Ehrlich, F. Abe, J. Nucl. Mater. 191–194 (1992) 116.
[6] J.S. Benjamin, Metall. Trans. 1 (1970) 2943.
[7] J.M. Poole, J.J. Fischer, G.A. J. Hack, G.M. McColvin, in: Advanced High Temperature Structural Materials and Protective Coatings, NRCC, Ottawa, Canada, 1994, p. 32.
[8] E. Arzt, R. Behr, E. Göhring, P. Grahle, R.P. Mason, Mater. Sci. Eng. A 234–236 (1997) 22.
[9] I.G. Wright, B.A. Wilcox, Metall. Trans. 5 (1974) 957.
[10] H. Nagai, Y. Takebayashi, H. Mitani, Metall. Trans. 12A (1981) 435.
[11] S. Ukai, M. Harada, H. Okada, M. Inoue, S. Nomura, S. Shikakura, K. Asabe, T. Nishida, M. Fujiwara, J. Nucl. Mater. 204 (1993) 65.
[12] A.V. Krajnikov, A.N. Demidik, H.M. Ortner, Mater. Sci. Eng. A 234–236 (1997) 357.
[13] G.R. Romanoski, L.L. Snead, R.L. Klueh, D.T. Hoelzer, J. Nucl. Mater. 283–287 (2000) 642.
[14] A.U. Seybolt, Trans. ASM 59 (1966) 860.
[15] T.A. Ramanarayanan, R. Ayer, R. Petkovic-Luton, D.P. Leta, Oxid. Met. 29 (1988) 445.
[16] B.A. Pint, A.J. Garratt-Reed, L.W. Hobbs, Mater. High Temp. 13 (1995) 3.
[17] B.A. Pint, Oxid. Met. 49 (1998) 531.
[18] B.A. Pint, P.F. Tortorelli, I.G. Wright, in: M. Schütze, W.J. Quadakkers (Eds.), Cyclic Oxidation of High Temperature Materials, The Institute of Materials, London, 1999, p. 111.
[19] B.A. Pint, J.M. Rakowski, NACE Paper #00-259, Houston, TX, presented at NACE Corrosion 2000, Orlando, FL, March 2000.
[20] B. Pieraggi, Oxid. Met. 27 (1987) 177.
[21] P.Y. Hou, J. Stringer, Mater. Sci. Eng. A 202 (1995) 1.
[22] M. Lambertin, G. Beranger, in: W. Embury (Ed.), High Temperature Oxidation and Sulfidation Processes, Canadian Institute of Metals, Ottawa, 1990, p. 93.
[23] W.J. Quadakkers, M.J. Bennett, Mater. Sci. Technol. 10 (1994) 126.
[24] A. Strawbridge, P.Y. Hou, Mater. High Temp. 12 (1994) 177.
[25] B.A. Pint, Oxid. Met. 45 (1996) 1.
[26] H. Asteman, J.-E. Svensson, M. Norell, L.-G. Johansson, Oxid. Met. 54 (2000) 11.
[27] D.T. Hoelzer, B.A. Pint, I.G. Wright, J. Nucl. Mater. 283–287 (2000) 1306.